ELSEVIER
Available online at www.sciencedirect.com
ScienceDirect
International Journal of Solids and Structures 43 (2006) 7919–7938
INTERNATIONAL JOURNAL OF SOLIDS and STRUCTURES
www.elsevier.com/locate/ijsolstr

Effective elastic properties of doubly periodic array of inclusions of various shapes by the boundary element method

C.Y. Dong

Department of Mechanics, School of Science, Beijing Institute of Technology, Beijing 100081, China

Received 5 September 2005; received in revised form 2 April 2006
Available online 22 April 2006

Abstract

A rectangular cell of known boundary conditions is cut out from a medium containing the doubly periodic array of inclusions. The stress and strain relationship of the rectangular cell is obtained by using the classical boundary element methods. By matching the boundary condition requirements, the effective elastic properties of the doubly periodic array of inclusions can then be calculated. Numerical examples from the sub-domain boundary element method and the single domain boundary element method are compared and discussed. However, the present method cannot be readily extended to domains having circular or curved boundary parts.

Keywords: Boundary element method; Doubly periodic inclusions; Effective elastic properties

1. Introduction

For media containing inclusions of various shapes, it is very difficult to obtain closed form solutions by the analytical methods, or an approximation by the numerical methods such as the finite element method and the boundary element method. Therefore, the simplified model (e.g. the regular distribution of multiple inclusions) has to be assumed so that a solution to the problems can be obtained using analytical or numerical methods. The application of Fourier series expansion method in doubly periodic inclusion problems can be found in the references, e.g. Nemat-Nasser and Hori (1999). However, it is not easy to determine the Fourier coefficient of the eigenstrain within periodic inclusions. The equivalent inclusion method (Eshelby, 1957) together with the results from doubly quasi-periodic Riemann boundary value problems (Lu, 1993) has been used to solve the doubly periodic cylindrical inclusion under longitudinal shear (Jiang et al., 2004). For other loading cases, e.g. tension, the implementation of their method might be quite complicated. The eigenfunction expansion variational method (Chen, 1983) was adopted to investigate doubly periodic circular holes in infinite plane (Chen and Lee, 2002). Nevertheless, it is still rather difficult to solve doubly periodic inclusion problems as all the above methods only tackle the inclusions of simple geometric shapes.

E-mail address: chunyingdong@yahoo.com

0020-7683/$ - see front matter
doi:10.1016/j.ijsolstr.2006.04.009

In this paper, a rectangular cell containing single or multiple inclusions is cut from a medium containing doubly periodic array of inclusions. The boundary condition on the rectangular cell is available for two loading systems, i.e. the tension and the in-plane shear. Thus, stress and displacement responses can be obtained using the sub-domain boundary element method and the single domain boundary element method. Based on these results, the elastic properties of the equivalent orthotropic medium can be achieved. The novelty of this paper is to combine the boundary element method and the rectangular cell model cut from a medium (Chen and Lee, 2002; Dong and Lee, 2005a) for a solution to the doubly periodic inclusion problems. The author is of the view that it might be difficult for the proposed method to be applied in a medium having circular or curved boundary parts. The reason is that the boundary conditions over these curved boundaries would be more complex.

2. Computational models

Fig. 1(a) shows a doubly periodic array of inclusions in an infinite plane medium subject to remote tension and in-plane shear forces. The geometry and the boundary conditions of two rectangular cells corresponding

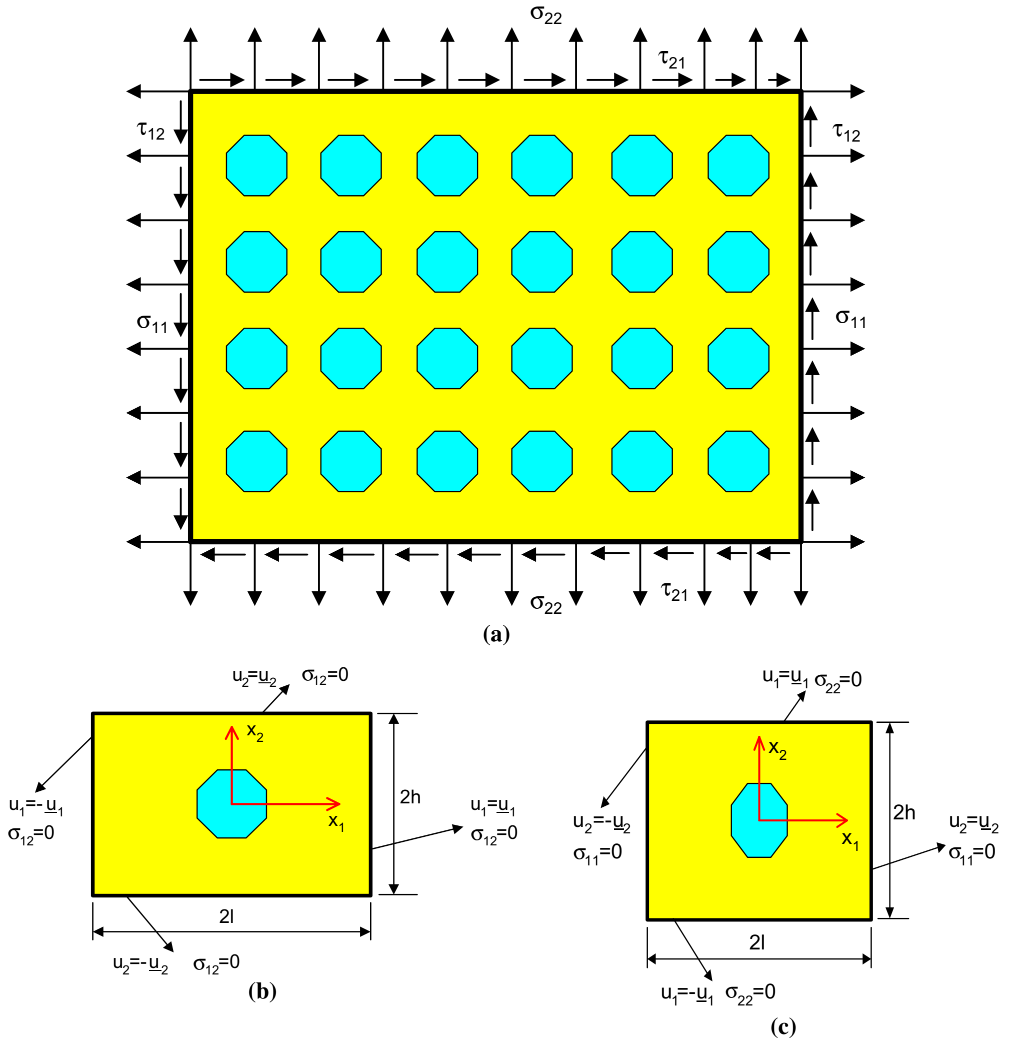

Fig. 1. (a) Doubly periodic inclusion problems; (b) rectangular cell containing single inclusion and its boundary condition for tension loading; (c) rectangular cell containing single inclusion and its boundary condition for shear force.

to remote tension and shear loadings are respectively shown in Fig. 1(b) and (c), in which $2l$ and $2h$ are respectively the edge lengths of the rectangular cells along directions x_1 and x_2.

Similar to 2D circular hole problems (Chen and Lee, 2002) and crack and rigid-line-inclusion problems (Dong and Lee, 2005a), the model as shown in Fig. 1(b) can be decomposed into two sub-models as shown in Fig. 2(a) and (b), each of which can be solved using the boundary element method presented in the next section. The equilibrium relationship of a cell of doubly periodic inclusion medium subject to a remote loading p along x_2 direction can be written as

$$u_{h2}\int_{-l}^{l} t_{2(2(a))}(x_1,h)\mathrm{d}x_1 + u_{l1}\int_{-l}^{l} t_{2(2(b))}(x_1,h)\mathrm{d}x_1 = 2lp \tag{1a}$$

$$u_{h2}\int_{-h}^{h} t_{1(2(a))}(l,x_2)\mathrm{d}x_2 + u_{l1}\int_{-h}^{h} t_{1(2(b))}(l,x_2)\mathrm{d}x_2 = 0 \tag{1b}$$

where u_{l1} and u_{h2} are respectively the displacements on the boundary $x_1 = l$ along direction x_1 and on the boundary $x_2 = h$ along direction x_2. $t_{1(2(a))}$ and $t_{1(2(b))}$ are the traction components on the boundary $x_1 = l$ along direction x_1 produced by sub-problems (2a) and (2b), respectively. $t_{2(2(a))}$ and $t_{2(2(b))}$ are the traction components on the boundary $x_2 = h$ along direction x_2 produced by sub-problems (2a) and (2b). The integrals in Eq. (1) and the following Eqs. (2) and (3) can be calculated using the trapezoidal rule of numerical integration (Scheid, 1988).

From Eq. (1), one can obtain u_{l1} and u_{h2}. Thus, the effective elastic properties E_2 and ν_{21} of doubly periodic inclusion problems can be calculated using Eq. (17) presented in Section 4.

Similarly, the equilibrium relationship of the cell of doubly periodic inclusion medium subject to a remote loading p along x_1 direction is given as follows

$$u_{h2}\int_{-l}^{l} t_{2(2(a))}(x_1,h)\mathrm{d}x_1 + u_{l1}\int_{-l}^{l} t_{2(2(b))}(x_1,h)\mathrm{d}x_1 = 0 \tag{2a}$$

$$u_{h2}\int_{-h}^{h} t_{1(2(a))}(l,x_2)\mathrm{d}x_2 + u_{l1}\int_{-h}^{h} t_{1(2(b))}(l,x_2)\mathrm{d}x_2 = 2hp \tag{2b}$$

Once u_{l1} and u_{h2} are solved by Eq. (2), the effective elastic properties E_1 and ν_{12} can be achieved using Eq. (19) presented in Section 4.

As the loading case shown in Fig. 1(c) can be decomposed into two sub-problems as shown in Fig. 3(a) and (b), the equilibrium relationship of the cell of doubly periodic medium subject to a remote shear loading p is given as follows

$$u_{h1}\int_{-l}^{l} t_{1(3(a))}(x_1,h)\mathrm{d}x_1 + u_{l2}\int_{-l}^{l} t_{1(3(b))}(x_1,h)\mathrm{d}x_1 = 2lp \tag{3a}$$

$$u_{h1}\int_{-h}^{h} t_{2(3(a))}(l,x_2)\mathrm{d}x_2 + u_{l2}\int_{-h}^{h} t_{2(3(b))}(l,x_2)\mathrm{d}x_2 = 2hp \tag{3b}$$

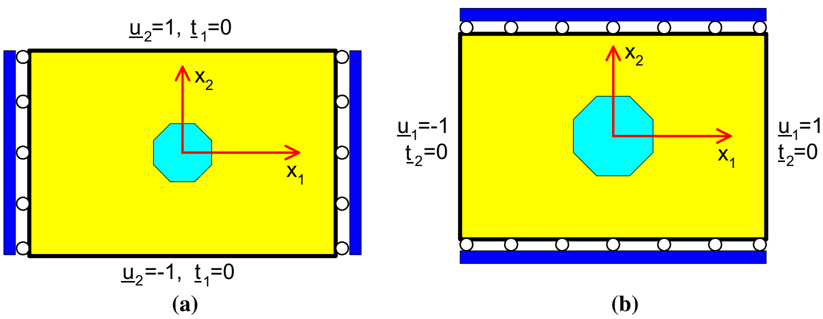

Fig. 2. Sub-problems from the boundary value problem as shown in Fig. 1(b).

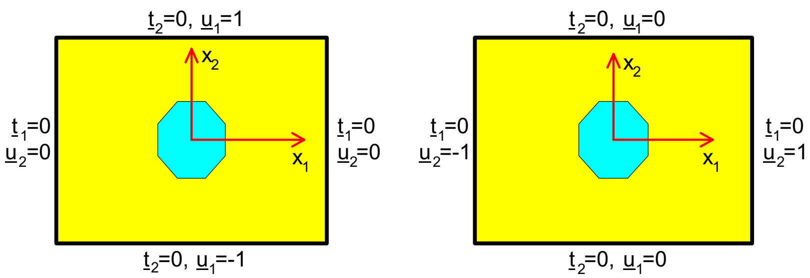

Fig. 3. Sub-problems from the boundary value problem as shown in Fig. 1(c).

where u_{l2} and u_{h1} are respectively the displacements on the boundary $x_1 = l$ along x_2 and on the boundary $x_2 = h$ along x_1 directions. $t_{1(3(a))}$ and $t_{1(3(b))}$ are the traction components on the boundary $x_2 = h$ along direction x_1 produced respectively by sub-problems (3a) and (3b), $t_{2(3(a))}$ and $t_{2(3(b))}$ are the traction components on the boundary $x_1 = l$ along direction x_2 produced respectively by sub-problems (3a) and (3b).

Once u_{l2} and u_{h1} are available, the effective shear modulus of doubly periodic inclusion problems can be obtained using Eq. (22) presented in Section 4.

3. Basic formulations

3.1. Sub-domain boundary element method

For the matrix and the inclusion, one can write their respective boundary integral equations as follows (Brebbia and Dominguez, 1992)

$$c_{ij}(p)u_j^{\mathrm{M}}(p) = \int_{\Gamma\cup\Gamma_c} U_{ij}^{\mathrm{M}}(p,q)t_j^{\mathrm{M}}(q)\mathrm{d}\Gamma(q) - \int_{\Gamma\cup\Gamma_c} T_{ij}^{\mathrm{M}}(p,q)u_j^{\mathrm{M}}(q)\mathrm{d}\Gamma(q) \tag{4}$$

and

$$c_{ij}(p)u_j^{\mathrm{I}}(p) = \int_{\Gamma_c} U_{ij}^{\mathrm{I}}(p,q)t_j^{\mathrm{I}}(q)\mathrm{d}\Gamma(q) - \int_{\Gamma_c} T_{ij}^{\mathrm{I}}(p,q)u_j^{\mathrm{I}}(q)\mathrm{d}\Gamma(q) \tag{5}$$

where $c_{ij}(p)$ can be determined indirectly using rigid body displacement method. Γ and Γ_c are respectively the outside and the inner boundaries of the matrix. The superscripts M and I denote respectively the matrix and the inclusion. U_{ij}^{α} and T_{ij}^{α} ($\alpha = \mathrm{M,I}$) are the fundamental solutions of 2-D elastic problems which are given as follows

$$U_{ij}^{\alpha} = \frac{1}{8\pi G^{\alpha}(1-\nu^{\alpha})}\left[(3-4\nu^{\alpha})\ln\left(\frac{1}{r}\right)\delta_{ij} + \frac{\partial r}{\partial x_i}\frac{\partial r}{\partial x_j}\right] \tag{6}$$

and

$$T_{ij}^{\alpha} = -\frac{1}{4\pi(1-\nu^{\alpha})r}\left[\frac{\partial r}{\partial n}\left\{(1-2\nu^{\alpha})\delta_{ij} + 2\frac{\partial r}{\partial x_i}\frac{\partial r}{\partial x_j}\right\} - (1-2\nu^{\alpha})\left(\frac{\partial r}{\partial x_j}n_i - \frac{\partial r}{\partial x_i}n_j\right)\right] \tag{7}$$

where G^{α} is the shear modulus and ν^{α} is Poisson's ratio. δ_{kl} is the Kronecker delta. $r_{,i} = \frac{\partial r(p,q)}{\partial x_i(q)}$ in which r is the distance between the field point q and the source point p. $\frac{\partial r}{\partial n} = r_{,i}n_i$ in which n_i is the directional cosine of the normal at the boundary point q with respect to x_i.

Eqs. (4) and (5) are discretized using quadratic boundary elements in which discontinuous quadratic boundary elements (see Fig. 4) are used near the corners of the inclusion–matrix interface. Considering the boundary condition of the matrix, one can obtain the following matrix forms (Dong et al., 2003)

$$\begin{bmatrix}\mathbf{B}_{11} & \mathbf{B}_{12}\\ \mathbf{B}_{21} & \mathbf{B}_{22}\end{bmatrix}\begin{Bmatrix}\mathbf{X}\\ \mathbf{U}_c^{\mathrm{M}}\end{Bmatrix} = \begin{Bmatrix}\mathbf{e}_1\\ \mathbf{e}_2\end{Bmatrix} + \begin{bmatrix}\mathbf{D}_1\\ \mathbf{D}_2\end{bmatrix}\{\mathbf{T}_c^{\mathrm{M}}\} \tag{8}$$

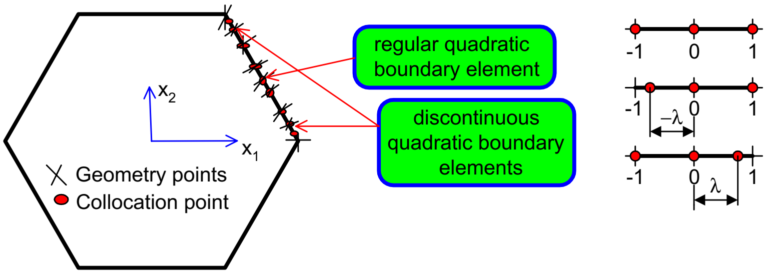

Fig. 4. The inclusion–matrix interface and reference system.

and

$$\mathbf{G}_c\mathbf{T}_c^{\mathrm{I}} = \mathbf{H}_c\mathbf{U}_c^{\mathrm{I}} \tag{9}$$

where $\mathbf{X}$ is the unknown vector over the boundary Γ of the matrix. $\mathbf{e}_1$ and $\mathbf{e}_2$ are the known vectors of the problem. $\mathbf{B}_{ij}$ $(i,j = 1,2)$, $\mathbf{D}_i$ $(i = 1,2)$, $\mathbf{G}_c$ and $\mathbf{H}_c$ are the associated coefficient matrices. The superscripts M and I represent respectively the matrix and the inclusion. $\mathbf{U}_c$ and $\mathbf{T}_c$ are respectively the displacement and traction vectors over the matrix–inclusion interface.

Based on the matrix–inclusion interface conditions for perfectly bonding, one can obtain the following system of equations

$$\begin{bmatrix} \mathbf{B}_{11} & \overline{\mathbf{B}}_{12} \\ \mathbf{B}_{21} & \overline{\mathbf{B}}_{22} \end{bmatrix} \begin{Bmatrix} \mathbf{X} \\ \mathbf{U}_c \end{Bmatrix} = \begin{Bmatrix} \mathbf{e}_1 \\ \mathbf{e}_2 \end{Bmatrix} \tag{10}$$

where $\overline{\mathbf{B}}_{12} = \mathbf{B}_{12} + \mathbf{D}_1\mathbf{G}_c^{-1}\mathbf{H}_c$ and $\overline{\mathbf{B}}_{22} = \mathbf{B}_{22} + \mathbf{D}_2\mathbf{G}_c^{-1}\mathbf{H}_c$.

Once $\mathbf{X}$ is available, the effective elastic properties of doubly periodic inclusion medium can be obtained based on the methods from Sections 2 and 4.

3.2. Simple domain boundary element method

It is assumed that the Poisson's ratios of the inclusions and the matrix are the same. Following the method presented by Leite et al. (2003) and Dong and Lee (2005b), we can obtain the following boundary integral equation formulations.

For the source point p outside of the matrix, we have

$$c_{ij}(p)u_j(p) = \int_\Gamma U_{ij}(p,q)t_j(q)\mathrm{d}\Gamma(q) - \int_\Gamma T_{ij}(p,q)u_j(q)\mathrm{d}\Gamma(q) - \int_{\Gamma_c}\left(1 - \frac{G^{\mathrm{I}}}{G}\right)T_{ij}(p,q)u_j(q)\mathrm{d}\Gamma \tag{11}$$

where $c_{ij}(p)$ can be determined indirectly using rigid body displacement method. Γ and Γ_c are respectively the outside and the inner boundaries of the matrix. The superscript I denote the inclusion. U_{ij} and T_{ij} are the fundamental solutions of 2-D elastic problems as shown in Eqs. (6) and (7).

When the source point p approaches the matrix–inclusion interface Γ_c, the following single-domain boundary integral equation holds

$$\left(1 + \frac{G^{\mathrm{I}}}{G}\right)c_{ij}(p)u_j(p) = \int_\Gamma U_{ij}(p,q)t_j(q)\mathrm{d}\Gamma(q) - \int_\Gamma T_{ij}(p,q)u_j(q)\mathrm{d}\Gamma(q) - \int_{\Gamma_c}\left(1 - \frac{G^{\mathrm{I}}}{G}\right)T_{ij}(p,q)u_j(q)\mathrm{d}\Gamma \tag{12}$$

where the kernels U_{ij} and T_{ij} have singularities of order ln(r) and r^{-1} respectively, which could be tackled by means of classical methods (Brebbia and Dominguez, 1992).

Following the conventional boundary element method (Brebbia and Dominguez, 1992), one can obtain the resulting system of equations from Eqs. (11) and (12)

$$\begin{bmatrix} \mathbf{A}_{11} & \mathbf{A}_{12} \\ \mathbf{A}_{21} & \mathbf{A}_{22} \end{bmatrix} \begin{Bmatrix} \mathbf{X} \\ \mathbf{U}_{\mathrm{c}} \end{Bmatrix} = \begin{Bmatrix} \mathbf{f}_1 \\ \mathbf{f}_2 \end{Bmatrix} \tag{13}$$

where $\mathbf{A}$ is the coefficient matrix, $\mathbf{X}$ is the vector of the unknowns of the outer boundary of the cell, $\mathbf{U}_{\mathrm{c}}$ is the displacement vector on the matrix–inclusion interface, $\mathbf{f}_1$ and $\mathbf{f}_2$ are the associated known values.

Notice that the traction equilibrium over the matrix–inclusion interface has been automatically satisfied using Eqs. (11) and (12). Therefore, compared with the sub-domain boundary integral equation approach (see Section 3.1), the single-domain boundary integral equation method presented in this section gives generally more accurate numerical results. The reason is due to the fact that the inverse matrix of the related matrix from the inclusion part must be calculated in the sub-domain boundary integral equation approach (Dong et al., 2003), while the single-domain boundary integral equation approach directly gives the resulting system of equations, i.e. Eq. (13). Furthermore, the single-domain boundary integral equation approach is especially suitable to solve the problems containing irregular inclusion shapes. The reason is that the corner problems encountered in the conventional boundary element methods have disappeared in this approach.

4. Effective elastic properties of the doubly periodic inclusion problems

Similar to doubly periodic hole problem (Chen and Lee, 2002) and doubly periodic crack and rigid-line-inclusion problems (Dong and Lee, 2005a), a medium containing doubly periodic array of inclusions of various shapes considered in this paper can also be considered as a homogeneous orthotropic medium, the constitutive relation of which is given as follows (Lekhnitskii, 1963)

$$\varepsilon_{11} = \frac{1}{E_1}\sigma_{11} - \frac{v_{21}}{E_2}\sigma_{22} \tag{14a}$$

$$\varepsilon_{22} = \frac{1}{E_2}\sigma_{22} - \frac{v_{12}}{E_1}\sigma_{11} \tag{14b}$$

$$\gamma_{12} = \frac{1}{G_{12}}\sigma_{12} \tag{14c}$$

In order to obtain the effective elastic properties E_2 and γ_{21}, the remote loading can be assumed as

$$\sigma_{11}^0 = 0 \tag{15a}$$

$$\sigma_{22}^0 = p \tag{15b}$$

$$\sigma_{12}^0 = 0 \tag{15c}$$

For the effective homogeneous orthotropic medium, its stress and strain states are given as follows

$$\overline{\sigma}_{11} = 0 \tag{16a}$$

$$\overline{\sigma}_{22} = p \tag{16b}$$

$$\overline{\sigma}_{12} = 0 \tag{16c}$$

$$\overline{\varepsilon}_{11} = \frac{u_{l1}}{l} \tag{16d}$$

$$\overline{\varepsilon}_{22} = \frac{u_{h2}}{h} \tag{16e}$$

where the bar over the above given symbols denotes the average value in unit cell. u_l and u_h are obtained from the single-domain or the sub-domain boundary integral equation approach based on the model as shown in Fig. 2.

Substituting Eq. (13) into Eq. (11), one can obtain

$$E_2 = \frac{ph}{u_{h2}} \tag{17a}$$

$$\nu_{21} = -\frac{hu_{l1}}{lu_{h2}} \tag{17b}$$

Similarly, when the remote loading is given as follows

$$\sigma_{11}^0 = p \tag{18a}$$

$$\sigma_{22}^0 = 0 \tag{18b}$$

$$\sigma_{12}^0 = 0 \tag{18c}$$

one can have

$$E_1 = \frac{pl}{u_{l1}} \tag{19a}$$

$$\nu_{12} = -\frac{lu_{h2}}{hu_{l1}} \tag{19b}$$

To find the effective shear modulus, the remote shear loading should be applied, i.e.

$$\sigma_{11}^0 = 0 \tag{20a}$$

$$\sigma_{22}^0 = 0 \tag{20b}$$

$$\sigma_{12}^0 = p \tag{20c}$$

For the effective homogeneous orthotropic medium, its stress and strain states corresponding to the remote shear loading are given as follows

$$\bar{\sigma}_{11} = 0 \tag{21a}$$

$$\bar{\sigma}_{22} = 0 \tag{21b}$$

$$\bar{\sigma}_{12} = p \tag{21c}$$

$$\bar{\varepsilon}_{12} = \frac{u_{l2}}{h} + \frac{u_{h1}}{l} \tag{21d}$$

Substituting Eq. (21) to Eq. (14c), one can obtain

$$G_{12} = \frac{p}{\left(\frac{u_{l2}}{h} + \frac{u_{h1}}{l}\right)} \tag{22}$$

For various doubly periodic inclusion problems, the corresponding effective elastic properties can be obtained from Eqs. (17), (19), and (22) using the boundary element method based on the computation models presented in Section 2.

5. Numerical examples

5.1. Doubly periodic circular holes

The doubly periodic circular holes in the matrix are considered as special doubly periodic circular inclusions of zero elastic modulus in the matrix. The radius of each circular hole is assumed to be R as shown in Fig. 5. The elastic modulus and Poisson's ratio of the medium are taken as $E^{\mathrm{M}} = 1$ and $\nu^{\mathrm{M}} = 0.3$, respectively.

This problem has been analyzed using the eigenfunction expansion variational method (Chen and Lee, 2002). In the present analysis, Poisson's ratio of the hole is assumed as 0.3, whilst the elastic modulus of the hole is taken as 0 and 10^{-10} in the single-domain and the sub-domain boundary element methods, respectively. The circular hole and each outside boundary are respectively discretized into 32 and 10 quadratic

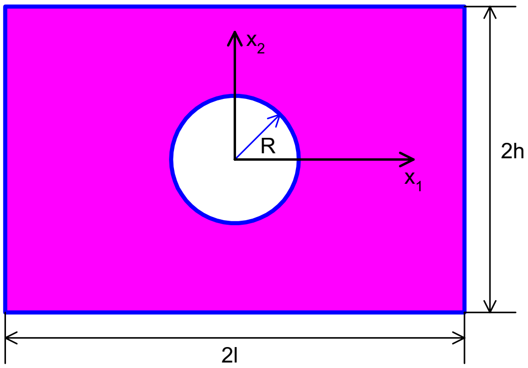

Fig. 5. Rectangular cell of doubly periodic circular holes.

Table 1
Normalized effective elastic modulus E_1/E^M

h/l	Methods	R/c							
		0.1	0.2	0.3	0.4	0.5	0.6	0.7	0.8
0.4	Present	0.9907	0.9635	0.9204	0.8636	0.7940	0.7114	0.6137	0.4964
	C&L	0.9907	0.9634	0.9203	0.8634	0.7938	0.7111	0.6135	0.4967
1.0	Present	0.9770	0.9139	0.8244	0.7244	0.6168	0.5117	0.4069	0.3000
	C&L	0.9770	0.9139	0.8244	0.7224	0.6168	0.5117	0.4069	0.3000
1.5	Present	0.9846	0.9422	0.8815	0.8118	0.7397	0.6683	0.5981	0.5287
	C&L	0.9846	0.9422	0.8815	0.8118	0.7397	0.6683	0.5981	0.5286

C&L denotes Chen and Lee (2002), $c = \min(l, h)$.

Table 2
Normalized effective elastic modulus E_2/E^M

h/l	Methods	R/c							
		0.1	0.2	0.3	0.4	0.5	0.6	0.7	0.8
0.4	Present	0.9908	0.9653	0.9288	0.8869	0.8435	0.8006	0.7583	0.7161
	C&L	0.9908	0.9653	0.9288	0.8868	0.8433	0.8002	0.7579	0.7160
1.0	Present	0.9770	0.9139	0.8244	0.7244	0.6168	0.5117	0.4069	0.3000
	C&L	0.9770	0.9139	0.8244	0.7224	0.6168	0.5117	0.4069	0.3000
1.5	Present	0.9845	0.9405	0.8737	0.7911	0.6977	0.5965	0.4887	0.3729
	C&L	0.9845	0.9404	0.8737	0.7911	0.6976	0.5965	0.4886	0.3730

C&L denotes Chen and Lee (2002), $c = \min(l, h)$.

Table 3
Normalized effective shear modulus G_{12}/G^M

h/l	Methods	R/c							
		0.1	0.2	0.3	0.4	0.5	0.6	0.7	0.8
0.4	Present	0.9903	0.9603	0.9080	0.8304	0.7251	0.5920	0.4357	0.2668
	C&L	0.9903	0.9603	0.9081	0.8309	0.7262	0.5945	0.4411	0.2800
1.0	Present	0.9759	0.9050	0.7916	0.6455	0.4826	0.3237	0.1884	0.0887
	C&L	0.9759	0.9049	0.7916	0.6454	0.4826	0.3237	0.1883	0.0886
1.5	Present	0.9839	0.9355	0.8552	0.7451	0.6107	0.4620	0.3125	0.1765
	C&L	0.9839	0.9355	0.8552	0.7451	0.6107	0.4622	0.3129	0.1777

C&L denotes Chen and Lee (2002), $c = \min(l, h)$.

Table 4
Effective Poisson' ratio

h/l	Poisson's ratio	R/c							
		0.1	0.2	0.3	0.4	0.5	0.6	0.7	0.8
0.4	ν_{12}	0.3002	0.3001	0.2974	0.2898	0.2754	0.2532	0.2227	0.1832
	ν_{21}	0.3003	0.3007	0.3001	0.2976	0.2926	0.2850	0.2753	0.2643
1.0	ν_{12}	0.3006	0.3010	0.2975	0.2867	0.2665	0.2365	0.1974	0.1506
	ν_{21}	0.3006	0.3010	0.2975	0.2867	0.2665	0.2365	0.1974	0.1506
1.5	ν_{12}	0.3005	0.3011	0.3001	0.2957	0.2868	0.2734	0.2561	0.2356
	ν_{21}	0.3004	0.3005	0.2974	0.2881	0.2705	0.2441	0.2092	0.1662

$c = \min(l, h)$.

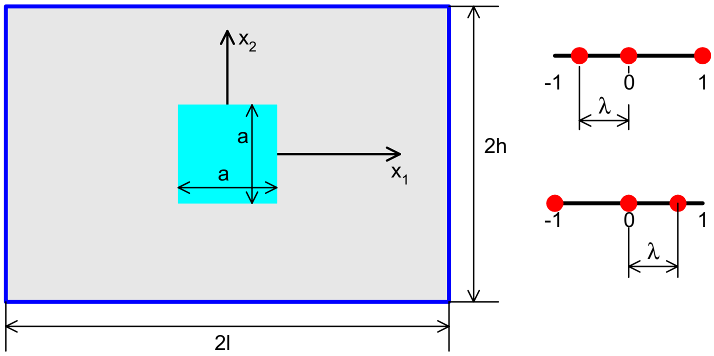

Fig. 6. Rectangular cell of doubly periodic square inclusions and reference system.

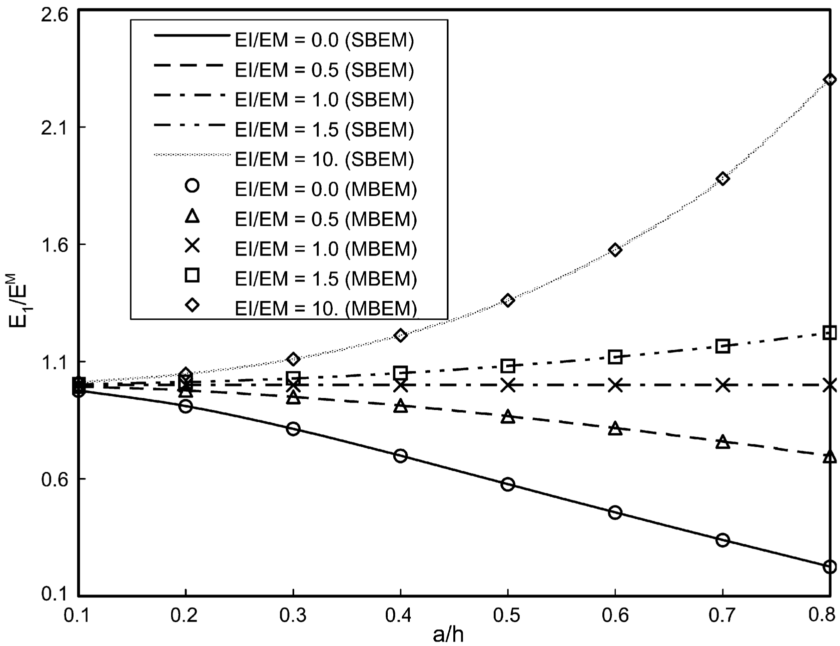

Fig. 7. Effective elastic modulus E_1 of doubly periodic square inclusions (SBEM – single domain boundary element method; MBEM – sub-domain boundary element method. SBEM and MBEM in the following figures contain the same meaning).

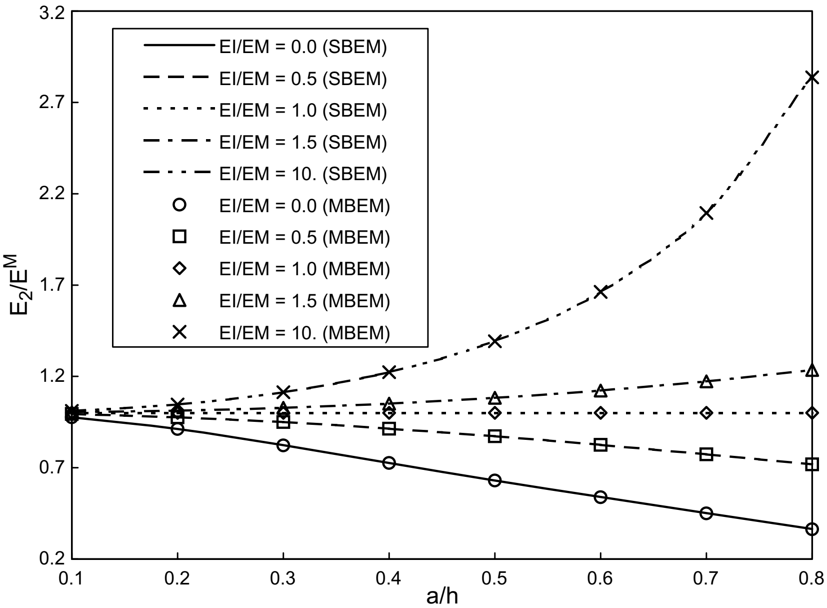

Fig. 8. Effective elastic modulus E_2 of doubly periodic square inclusions.

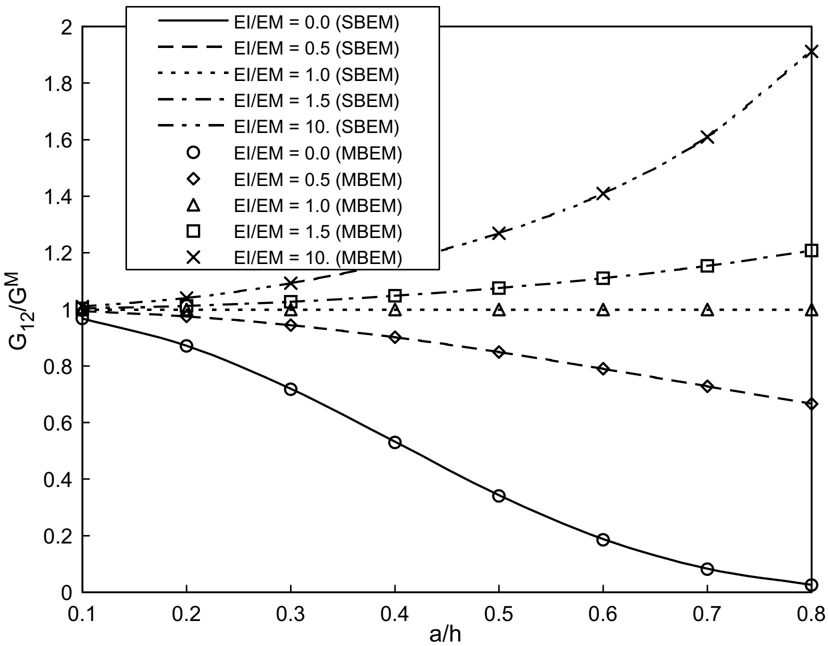

Fig. 9. Effective shear elastic modulus G_{12} of doubly periodic square inclusions.

boundary elements for various cases. Effective elastic properties of the double periodic circular hole problem are obtained using the single-domain and the sub-domain boundary element methods and shown in Tables 1–3 in which results from Chen and Lee (2002) are also listed. One can find that the results from the

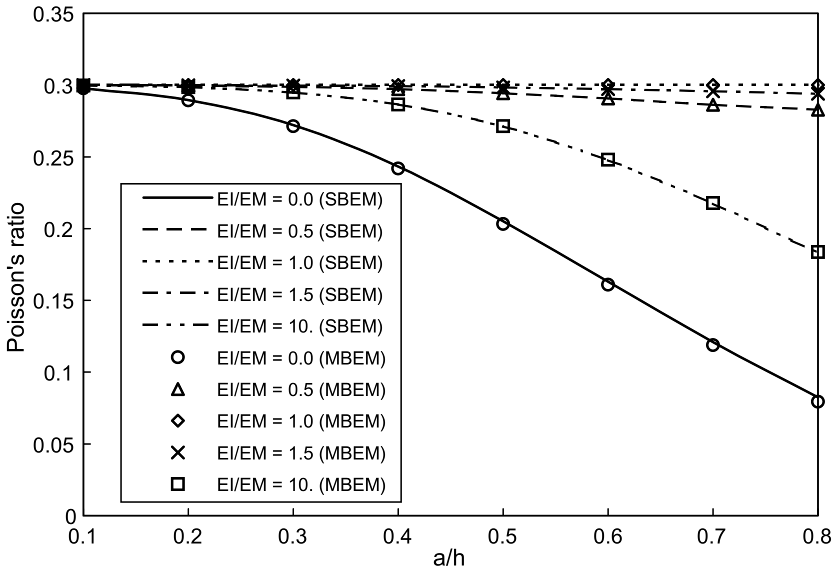

Fig. 10. Effective Poisson's ratio v_{12} of doubly periodic square inclusions.

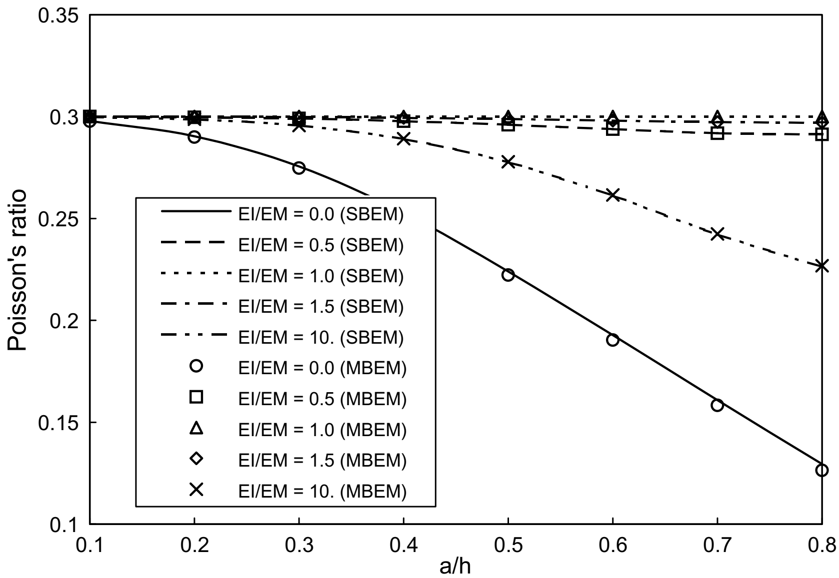

Fig. 11. Effective Poisson's ratio v_{21} of doubly periodic square inclusions.

single-domain and the sub-domain boundary element methods are in excellent agreement with those of Chen and Lee (2002). The relationship of $E_1 v_{21}/(E_2 v_{12}) = 1$ is well approximated using the obtained data as shown in Tables 1, 2 and 4. This relationship was also obtained by Chen and Lee (2002). Note that the results from the single-domain boundary element method (SBEM) are the same as those from the sub-domain boundary element method (MBEM) up to four decimal places, except for $h/l = 0.4$ and $R/c = 0.2$, $E_1/E^{\mathrm{M}} = 0.9636$ (SBEM) and 0.9635 (MBEM), and for $h/l = 1.5$ and $R/c = 0.8$, $v_{21} = 0.1661$ (SBEM) and 0.1662 (MBEM).

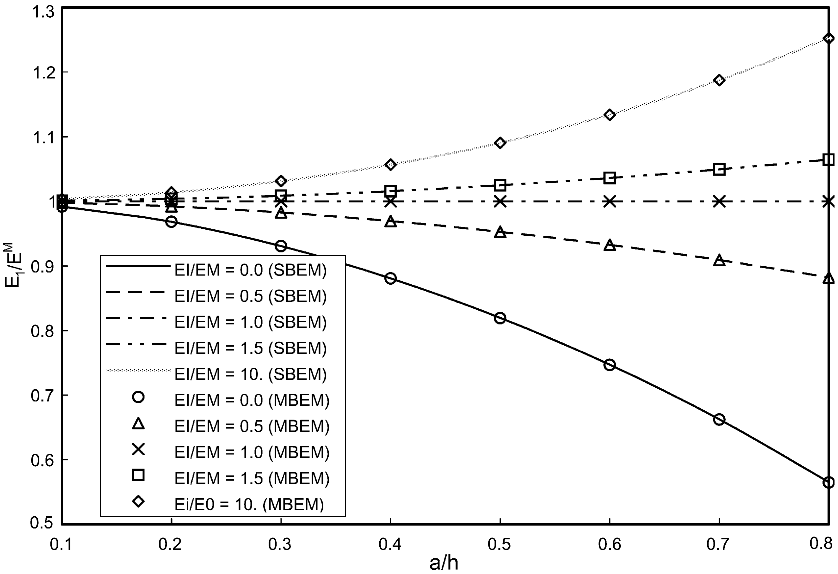

Fig. 12. Effective elastic modulus E_1 of doubly periodic hexagonal inclusions.

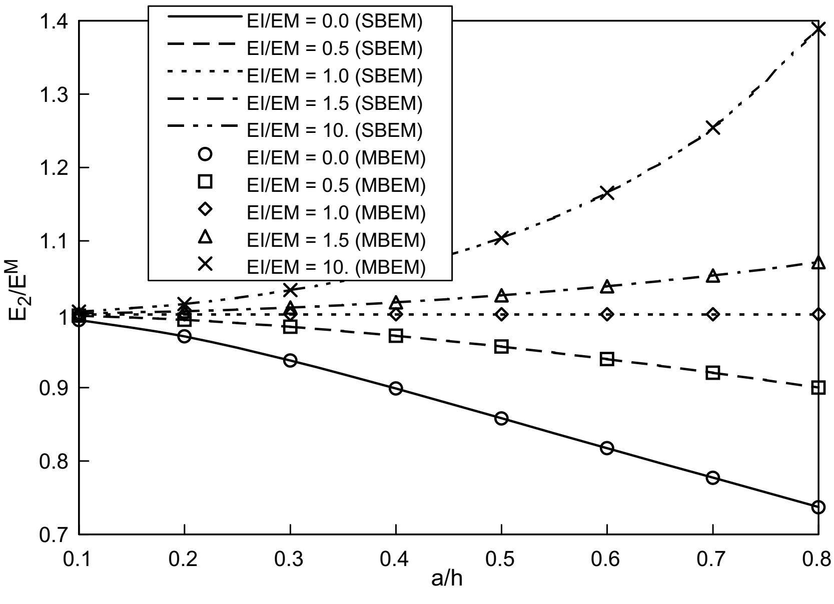

Fig. 13. Effective elastic modulus E_2 of doubly periodic hexagonal inclusions.

5.2. Doubly periodic square inclusions

Geometric data of the cell of a doubly periodic square inclusions is taken as $h/l = 0.8$, and the side length a of square inclusions can be varied. The elastic modulus and the Poisson's ratio of the matrix are denoted as $E^{\mathrm{M}} = 1$ and $v^{\mathrm{M}} = 0.3$. The elastic modulus and the Poisson's ratio of the inclusion are taken as E^{I} and $v^{\mathrm{I}} = v^{\mathrm{M}} = 0.3$, respectively.

Each boundary of the rectangular cell and each side of the square inclusion is meshed into 10 quadratic boundary elements. Discontinuous quadratic boundary elements ($\lambda = 0.95$, see Fig. 6) are used near the

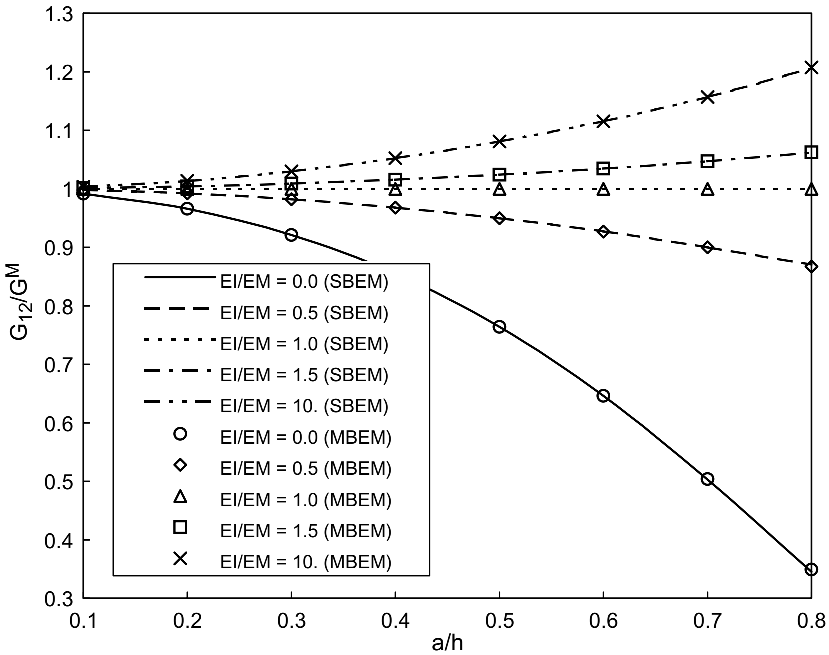

Fig. 14. Effective shear modulus G_{12} of doubly periodic hexagonal inclusions.

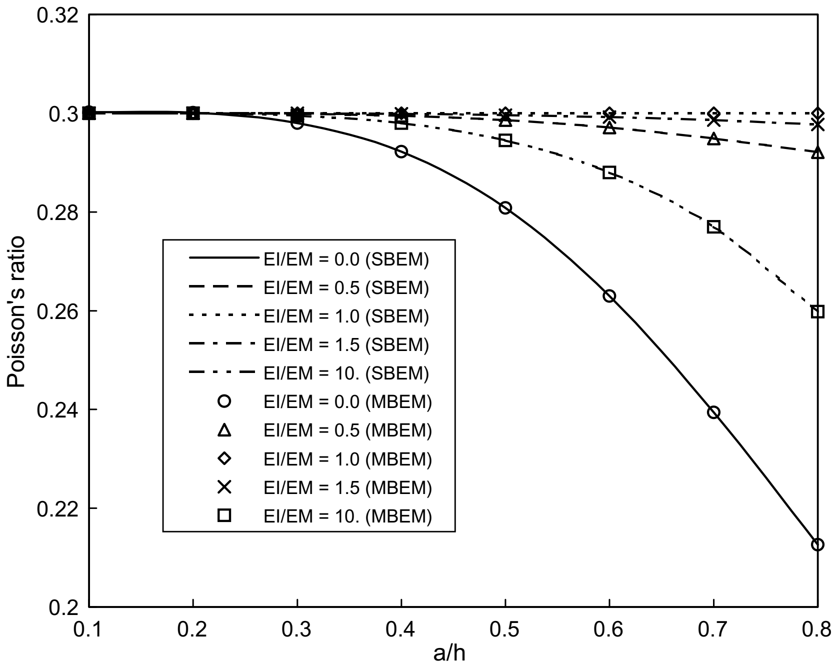

Fig. 15. Effective Poisson's ratio v_{12} of doubly periodic hexagonal inclusions.

corners of square inclusion in the numerical implementation of the sub-domain boundary element method. Effective elastic properties of the medium for various square inclusions are shown in Figs. 7–11. One can

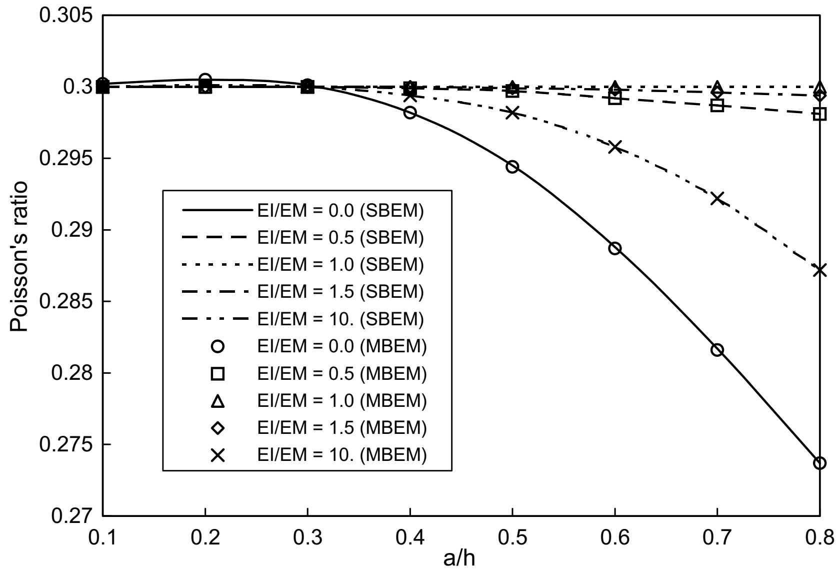

Fig. 16. Effective Poisson's ratio v_{21} of doubly periodic hexagonal inclusions.

observe that the results from the sub-domain boundary element method and the single domain boundary element method are in good agreement with each other.

5.3. Doubly periodic regular hexagonal inclusions

Geometric data of a typical cell of doubly periodic regular hexagonal inclusions is taken as $h/l = 0.4$, and the side length a of the hexagonal inclusion can be varied. The elastic modulus and the Poisson's ratio of the matrix are denote as $E^M = 1$ and $v^M = 0.3$. The elastic modulus and the Poisson's ratio of the inclusion are taken as E^I and $v^I = v^M = 0.3$, respectively.

Each boundary of the rectangular cell and each side of the hexagonal inclusion is meshed into 10 quadratic boundary elements. Discretized into 10 quadratic boundary elements in which the discontinuous quadratic boundary elements ($\lambda = 0.95$, see Fig. 4) are used near the corners of regular hexagonal inclusion in the numerical implementation of the sub-domain boundary element method. Effective elastic properties of the medium for various regular hexagonal inclusions are shown in Figs. 12–16. Similar to the last example, one can observe

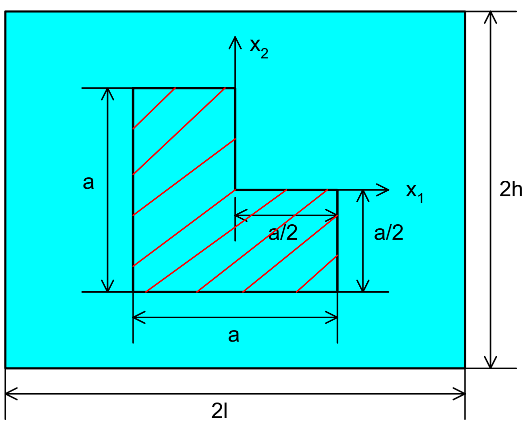

Fig. 17. A cell of doubly periodic irregular inclusions.

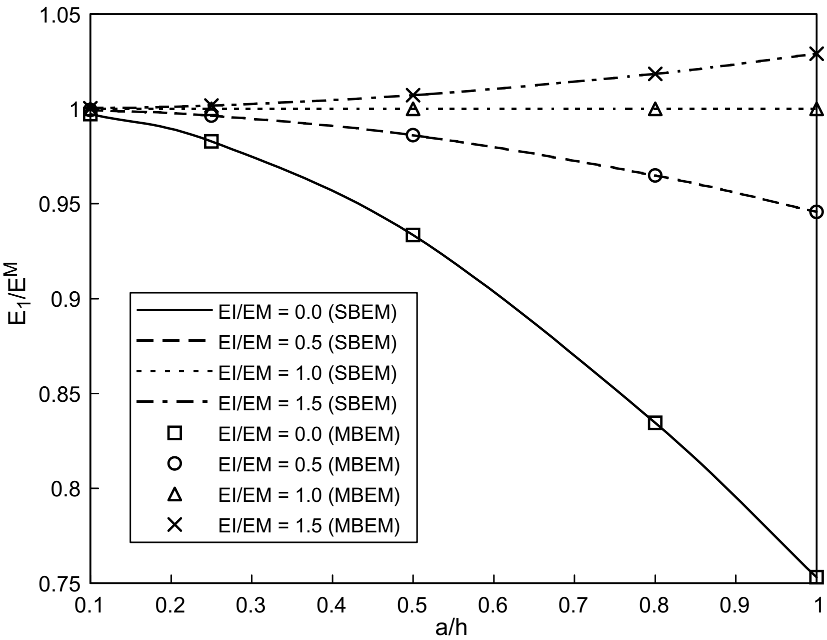

Fig. 18. Effective elastic modulus E_1 of doubly periodic irregular inclusions.

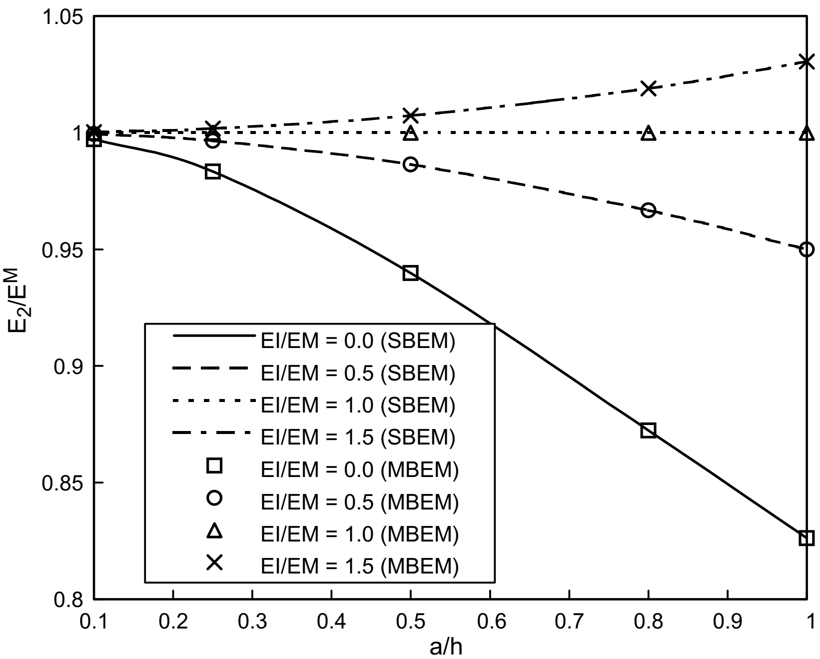

Fig. 19. Effective elastic modulus E_2 of doubly periodic irregular inclusions.

that the results from the sub-domain boundary element method and the single domain boundary element method are also in good agreement with each other.

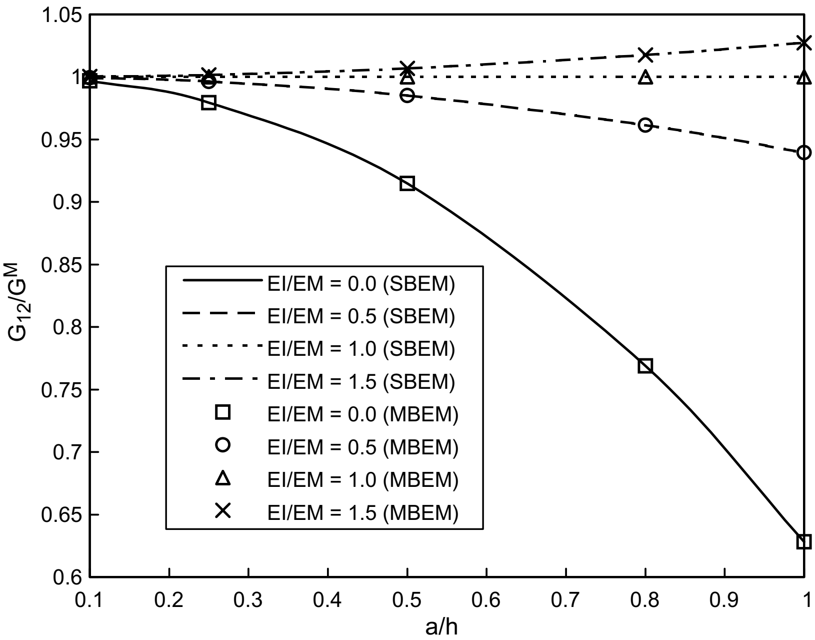

Fig. 20. Effective shear modulus G_{12} of doubly periodic irregular inclusions.

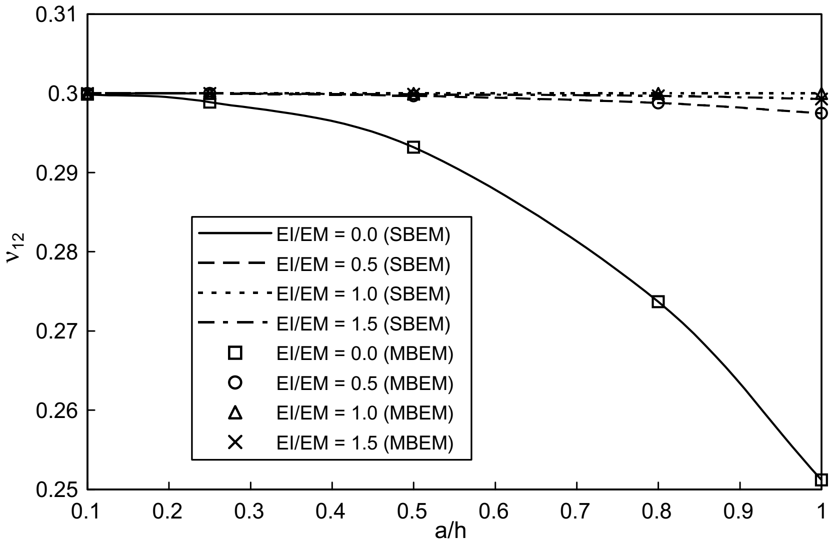

Fig. 21. Effective Poisson's ratio v_{12} of doubly periodic irregular inclusions.

5.4. Doubly periodic irregular inclusions

Geometric data of a typical cell of doubly periodic irregular inclusions as shown in Fig. 17 is taken as $h/l = 0.4$, and the length a of irregular inclusion is changed. The elastic modulus and the Poisson's ratio of the matrix are denoted as $E^{\mathrm{M}} = 1$ and $v^{\mathrm{M}} = 0.3$. The elastic modulus and the Poisson's ratio of the inclusion are taken as E^{I} and $v^{\mathrm{I}} = v^{\mathrm{M}} = 0.3$, respectively.

Each boundary of the rectangular cell and each side of the inclusion is meshed into 10 quadratic boundary elements. Discontinuous quadratic boundary elements are used near the corners of the inclusion in the numer-

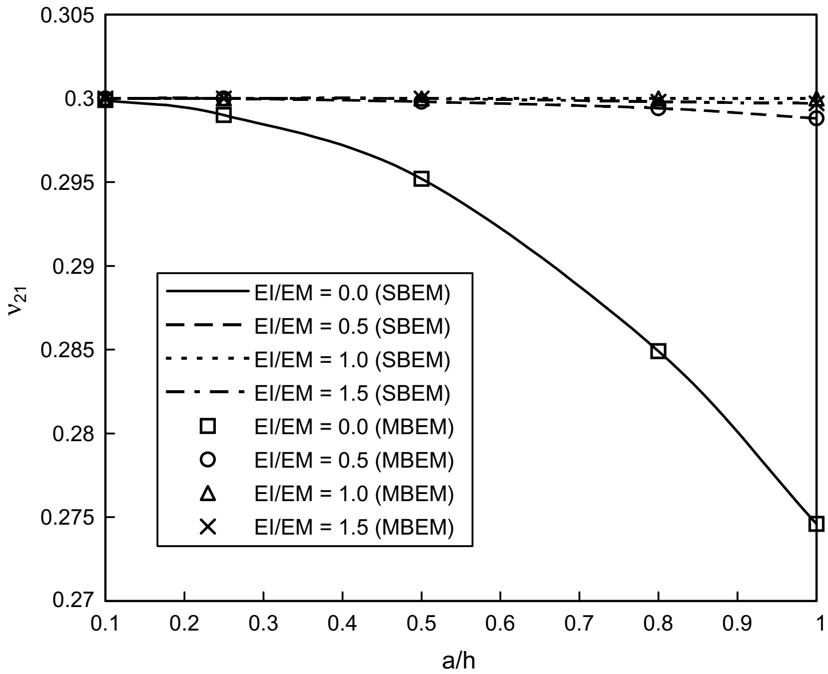

Fig. 22. Effective Poisson's ratio ν_{21} of doubly periodic irregular inclusions.

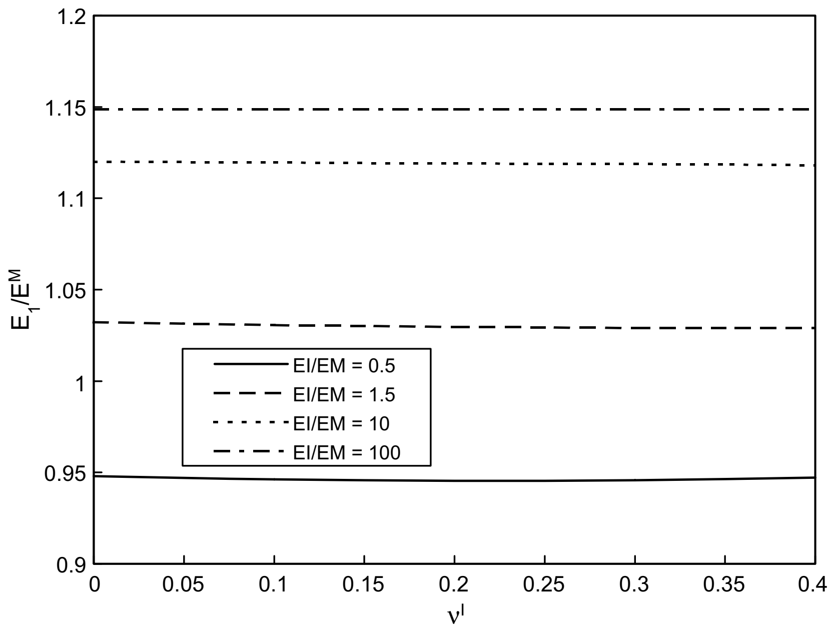

Fig. 23. Effective elastic modulus E_1 of doubly periodic irregular inclusions for various ν^{I}.

ical implementation of the sub-domain boundary element method. Effective elastic properties of the medium for the inclusion with different lengths a are shown in Figs. 18–22. Similar to the previous examples, one can observe that the results from the sub-domain boundary element method and the single domain boundary element method are also in good agreement with each other.

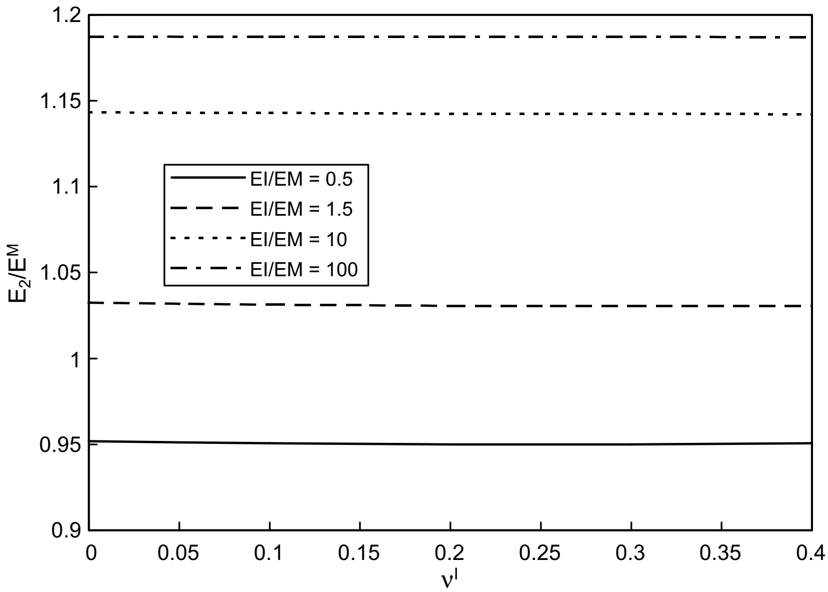

Fig. 24. Effective elastic modulus E_2 of doubly periodic irregular inclusions for various v^{I}.

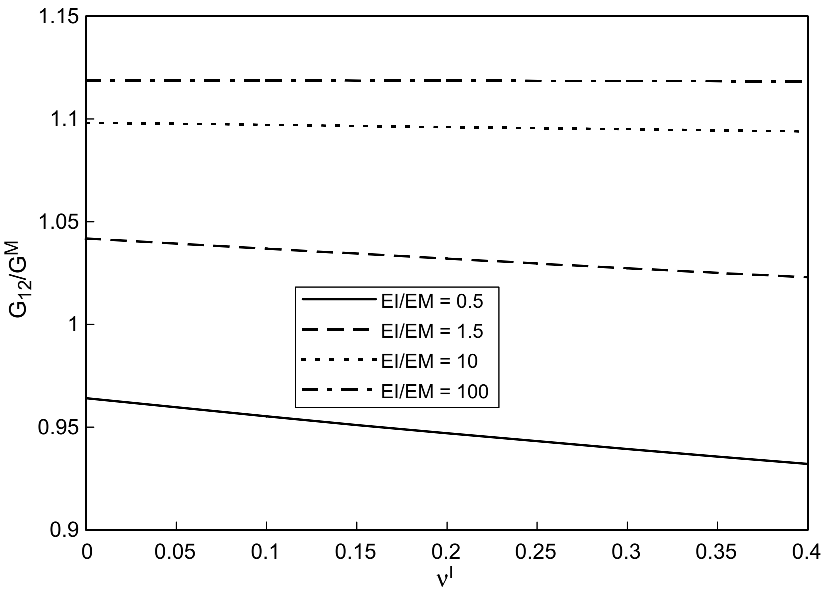

Fig. 25. Effective shear modulus G_{12} of doubly periodic irregular inclusions for various v^{I}.

For the Poisson's ratio of the inclusion being different from that of the matrix, some results for $a/h = 1$, $E^{\mathrm{I}}/E^{\mathrm{M}} = 0.5$, $E^{\mathrm{I}}/E^{\mathrm{M}} = 1.5$, $E^{\mathrm{I}}/E^{\mathrm{M}} = 10$ and $E^{\mathrm{I}}/E^{\mathrm{M}} = 100$ are shown in Figs. 23–27, respectively. These results are obtained using the sub-domain boundary element method. One can find that the effect of Poisson's ratio on the effective elastic moduli E_1 and E_2 can be ignored, but the effect of Poisson's ratio on the effective elastic shear modulus G_{12} and the effective Poisson's ratios v_{12} and v_{21} is quite significant. However, with the increase of the inclusion elastic modulus, the effect of Poisson's ratio on effective elastic properties becomes less and

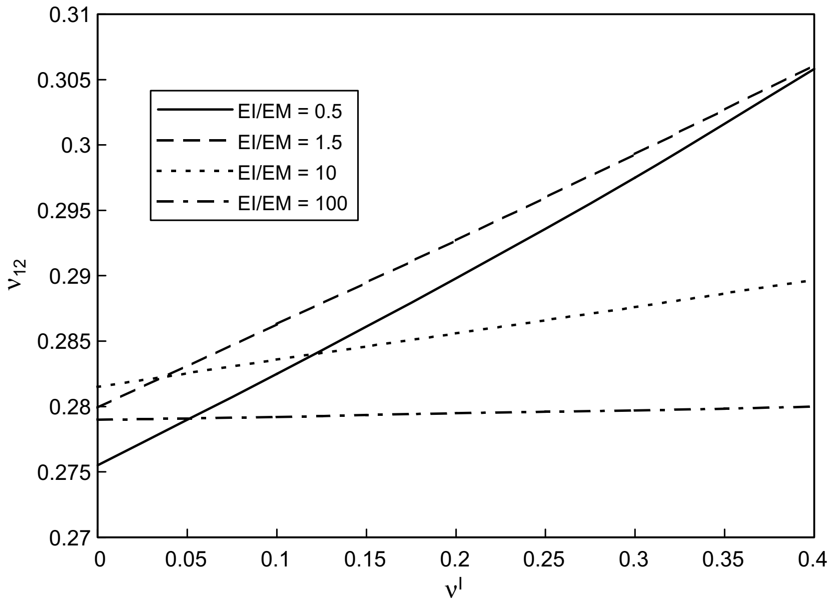

Fig. 26. Effective Poisson's ratio ν_{12} of doubly periodic irregular inclusions for various ν^I.

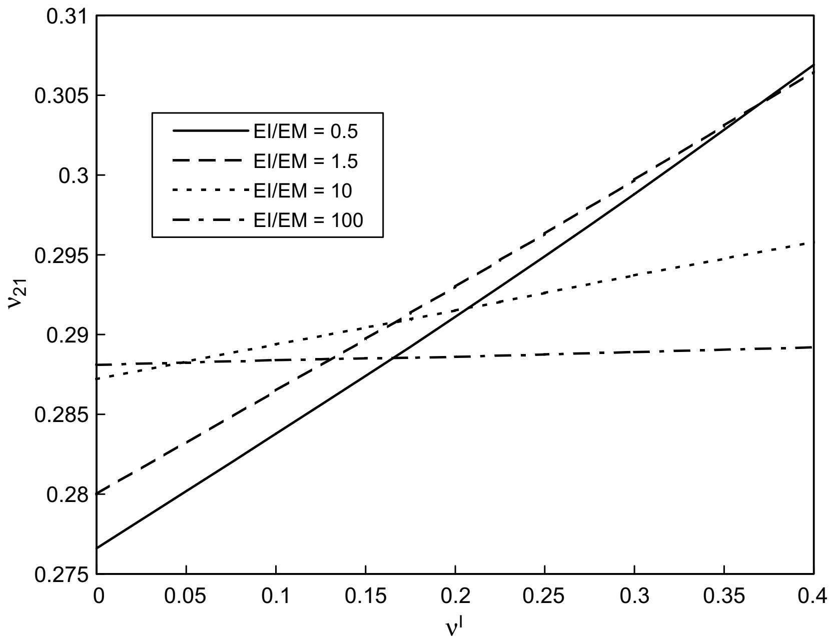

Fig. 27. Effective Poisson's ratio ν_{21} of doubly periodic irregular inclusions for various ν^I.

less. Thus, for hard inclusions, the single domain boundary element method can also be applied to inclusion problems having different Poisson's ratios for the inclusion and the matrix. Note that for $\nu^{\mathrm{I}} = \nu^{\mathrm{M}} = 0.3$, similar to the previous examples, the results from the single-domain boundary element method are the same as those from the sub-domain boundary element method for four decimal places.

6. Conclusions

By means of the sub-domain and the single domain boundary element methods, the effective elastic properties of doubly periodic array of various inclusion problems have been obtained. For doubly periodic circular hole problems, the present results are in excellent agreement with the results available, whilst for the other inclusion problems, the results from the sub-domain and the single domain boundary element methods are in good agreement with each other. For harder inclusion problems with different Poisson's ratios for the inclusion and the matrix, the single domain boundary element method can produce promising results compared with the sub-domain boundary element method. The numerical results presented in the paper can be considered as benchmark results for future research. It should be noted that the present method cannot be readily applied to media having circular or curved boundary parts due to the complex boundary conditions involved.

Acknowledgements

The work described in this paper was partially supported by the Research Fundamental Funding of Beijing Institute of Technology, China. The author would like to thank two anonymous reviewers and Professor D.A. Hills for their constructive comments and suggestions on the paper. The comments of Professor S.H. Lo at the Department of Civil Engineering of the University of Hong Kong and Professor Yunhui Zhang at Bohai University, China, are also appreciated.

References

Brebbia, C.A., Dominguez, J., 1992. Boundary Elements – An Introduction Course. Computational Mechanics Publications, Southampton.

Chen, Y.Z., 1983. An investigation of the stress intensity factors for a finite internally cracked plate by using variational method. Engineering Fracture Mechanics 17, 387–394.

Chen, Y.Z., Lee, K.Y., 2002. Two-dimensional elastic analysis of doubly periodic circular holes in infinite plane. KSME International Journal 1 (5), 655–665.

Dong, C.Y., Lee, K.Y., 2005a. Numerical analysis of doubly periodic array of cracks/rigid-line inclusions in an infinite isotropic medium using the boundary integral equation method. International Journal of Fracture 133 (4), 389–405.

Dong, C.Y., Lee, K.Y., 2005b. A new integral equation formulation of two-dimensional inclusion-crack problems. International Journal of Solids and Structures 42 (18–19), 5010–5020.

Dong, C.Y., Lo, S.H., Cheung, Y.K., 2003. Stress analysis of inclusion problems of various shapes in an infinite anisotropic elastic medium. Computational Methods and Applications in Mechanical Engineering 192 (5–6), 685–698.

Eshelby, J.D., 1957. The determination of the elastic field of an ellipsoidal inclusion, and related problems. Proceedings of the Royal Society of London, Series A 241, 371–396.

Jiang, C.P., Xu, Y.L., Cheung, Y.K., Lo, S.H., 2004. A rigorous analytical method for doubly periodic cylindrical under longitudinal shear and its application. Mechanics of Materials 36, 225–237.

Leite, L.G.S., Coda, H.B., Venturini, W.S., 2003. Two-dimensional solids reinforced by thin bars using the boundary element method. Engineering Analysis with Boundary Elements 27, 193–201.

Lekhnitskii, S.G., 1963. Theory of Elasticity of an Anisotropic Elastic Body. Holden-Day.

Lu, J.K., 1993. Boundary Value Problems for Analytic Functions. World Scientific, Singapore.

Nemat-Nasser, S., Hori, M., 1999. Micromechanics: Overall Properties of Heterogeneous Materials. Elsevier Science, Amsterdam.

Scheid, F., 1988. Schaum's Outline of Theory and Problems of Numerical Analysis. McGraw-Hill Book Company, New York.